

SULI Report: UEDGE simulations of a direct fusion drive FRC rocket

Nick McGreivy

(Dated: September 2016)

The field-reversed configuration (FRC) is being considered for use as a terrestrial power plant and as a direct-fusion-drive rocket engine for future space missions in the solar system. To produce thrust for a rocket or extract energy for electricity production, an asymmetric SOL has been proposed in which coolant/propellant gas is injected into a gas box at one end of the SOL. Plasma formed in the gas box flows along the SOL and its electrons are heated as they pass near the FRC core. The heated plasma is then ejected out a magnetic nozzle at the opposite end. We have used a 2D fluid code, UEDGE, to conduct numerical simulations of this FRC's SOL. We have examined the effects of power input from the FRC core (1-4 MW) and gas flow into the gas box (0.01-0.5 grams per second) on the rockets thrust (2-50 N) and specific impulse (ca. $1.5e4$ s) as well as on the power flow within the SOL. One important result is that the high plasma flow out of the gas box and the cold plasma within it reduce the power flow into the gas box well below 50% of the input power. Plasma dynamics of the gas box region have been investigated to assess the degree of detachment that can be obtained for given performance requirements. Finally, an FRC is evaluated for performance as a direct-fusion-drive rocket engine.

This is the "research report paper" required as part of the SULI program. My goal with this report is to introduce future students to this research project, so that any students whose work will build upon this project will understand the project and it's results. The intended audience of this report is therefore either a new summer intern or a second-year graduate student. If any reader has a question regarding this project or regarding UEDGE, or is hoping for any sort of clarification or explanation, feel free to email nickmcgreivy@gmail.com and I'll do my best to answer.

I. INTRODUCTION

A. Field reversed configuration

The field-reversed configuration (FRC) is being studied for use as a fusion reactor. The FRC has many advantages relative to other reactor designs, including compact size, smaller neutron flux, high β (ratio of plasma pressure to magnetic field pressure), and the potential to be used as a rocket engine.

Figure 1 shows a schematic of an FRC. The closed field lines in the center of figure 1 are the core. In this case, the closed field lines are generated by odd-parity rotating magnetic fields. The open field lines surrounding the core are known as the scrape-off layer (SOL). Fusion power is generated in the core of the FRC. Some of this energy is deposited via the fusion products in the SOL via electron heating⁵. The shaded region in the left of figure 1 is the gas box. Here, cold gas is puffed into the gas box. This gas will eventually become ionized, flow through the SOL, and out a magnetic nozzle, which is shown in the right of figure 1.

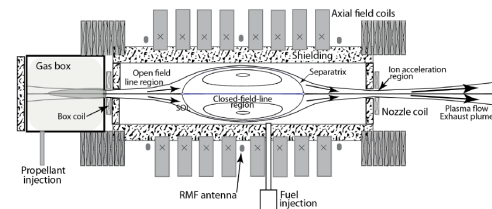


FIG. 1. A schematic of a field-reversed configuration.

B. Rocket applications

Chemical rockets have relatively low specific impulse, and are thus too slow to be used for most manned missions within the solar system. In addition, Wurden¹ clearly explains the need to develop a high-speed rocket for planetary defense. There is a need for a high thrust, high specific-impulse rocket engine. An FRC has been proposed as such a rocket engine. Because of its small size, linear design, intrinsic power generation, and high exhaust velocity, an FRC could serve as both the engine and power source for a manned or unmanned rocket for missions within the space system.

A simplified model of the FRC rocket is as follows: gas which is input into the gas box becomes ionized as it moves closer to the core. Once it is ionized, the plasma flows along the field lines of the SOL. As the plasma flows around the core, the electrons are heated⁵ by the fusion power. At the magnetic nozzle, the hot electrons setup an electric field in the nozzle, which accelerates the protons out the nozzle. Once it leaves the nozzle, the ejected plasma detaches from the magnetic field lines. The thrust can be calculated from the exhaust velocity of the particles from the FRC and the mass flow rate out the open end.

1. Rocket equations

The following equations apply to simple rockets. T is the thrust, η is the propulsion efficiency, I_{sp} is the specific impulse, g is the gravitational acceleration at the surface of the earth, \dot{m} is the mass flow rate, P is the power input from the core, and v is the exhaust velocity of the rocket.

The equation for T is as follows:

$$T = \dot{m}v_{\parallel} \quad (1)$$

The equation for I_{sp} is as follows:

$$I_{sp} = \frac{T}{\dot{m}g} \quad (2)$$

The equation for η is as follows:

$$\eta = \frac{\dot{m}v_{\parallel}^2}{2P} \quad (3)$$

η is defined as the ratio of the power going into the parallel kinetic energy of the particles leaving the FRC to the power input into the SOL.

C. Scrape off layer

As previously mentioned, the SOL is the region of open field lines surrounding the core of an FRC. In this region, fusion power from the core is deposited in the electrons. Clearly, in steady-state this power must be transported out of the FRC. Some of this power will be transported out of the magnetic nozzle of the FRC, some of this power will be transported to the walls of the gas box, and some of this power will be transported to the outer wall of the FRC. Energy that flows out of the magnetic nozzle will provide thrust; energy that flows to material surfaces could be recovered through a thermal cycle and converted, with an efficiency of 30-60%, into electricity. For rocket applications, it is preferred that most energy deposited into the SOL would flow out the magnetic nozzle.

Detachment is a possible state of plasma near a plasma-wall interface. Although it is not precisely defined, detachment is associated with low power and ion flux to the wall as well as a large pressure gradient along the magnetic field line. Typically, detachment is desirable, as it spreads the power flux over larger sections of the gas box walls and reduces the energy of the plasma ions, electrons, and neutrals that hit those surfaces.

D. UEDGE code

UEDGE is a 2D multi-species fluid code used to model the SOL region of fusion reactors. UEDGE was used to conduct the simulations presented in this report, and is

therefore important both to this project and the work of any future students. UEDGE finds a steady-state self-consistent solution to continuity equations, momentum equations, and energy equations for each species. The equations and transport coefficients are taken from Braginskii⁶. UEDGE also calculates ionization and recombination rates, and has scripts to calculate the flow of power and particles in a simulation.

To any students working in UEDGE, be sure to get a copy of the UEDGE manual and use that as a guide for technical difficulties. Often, your question will not be discussed in that manual, so get a copy of the UEDGE source code and figure out a way to grep for the relevant information.

E. My project

The first goal of my project was to investigate the scrape-off layer of an FRC using UEDGE. This included determining the SOL parameters (temperature, density, velocity, etc) and power flow within the SOL, each as a function of heating power and gas input. It also included assessing the degree of detachment obtained for varying inputs. The second goal of my project was to evaluate the performance of an FRC as a direct-fusion-drive rocket engine. This included determining typical values of thrust, efficiency, and specific impulse (exhaust velocity) as a function of heating power and gas input.

F. Relevant previous work

Matt Chu Cheong, a previous summer intern, conducted a similar analysis for a one-dimensional geometry⁸. My project is the first comprehensive two-dimensional multi-fluid simulation of the entire SOL of an FRC with a gas box divertor at one end, evaluating the specific impulse, thrust, and efficiency of the proposed PFRC direct-fusion-drive rocket.

II. METHODS

Figure 2 shows the magnetic geometry used in each of these UEDGE simulations. This 2-dimensional image represents a slice of constant ϕ of a cylindrically symmetric FRC SOL. The simulation models the SOL under the assumption that the FRC core is generating fusion power. The left of the image represents the gas box, the right of the image represents the magnetic nozzle and expansion region, and the center of the image represents the SOL field lines surrounding the core. The red arrows show where the fusion products are expected to deposit energy in a FRC reactor as well as where power is deposited in the electrons in this simulation. The blue arrows point to where deuterium gas is puffed into the simulation. There

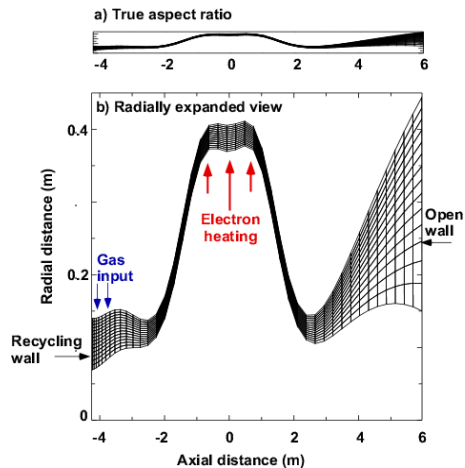


FIG. 2. UEDGE uses this magnetic geometry for these simulations. (a) gives the true aspect ratio of the simulation, while (b) is a radially expanded view.

are 46 gridpoints in the axial direction (z) and 16 gridpoints in the radial direction (r).

Deuterium plasma is used in this simulation, along with two types of deuterium gas: atomic deuterium (D) and molecular deuterium (D_2). Molecular deuterium is what is puffed into the simulation. UEDGE allows for a molecule to dissociate into two atomic deuterium. When this happens, $10eV$ is transferred from the electron thermal energy into the ion/atomic neutral thermal energy. This value of $10eV$ could be changed using *ediss* and *eion*. When an atomic deuterium is ionized, $13.6eV$ is taken from the electron channel. When a deuterium ion recombines, $13.6eV$ is radiated as a photon.

A. Simulation boundary conditions

The right boundary is an open boundary where particles are allowed to flow unimpeded out of the simulation, and gradients in density and temperature are zero. This is physically applicable to an FRC rocket, where the boundary at the magnetic nozzle is the vacuum of space. The left boundary represents one wall of the gas box wall. Here, 99.9% of the incoming deuterium ions and atomic deuterium is recycled off the wall as molecular deuterium. The thermal flux and (ionization) potential energy of the plasma ions are deposited onto the gas box walls. The plasma is allowed to stream freely to the wall, but the atomic deuterium is constrained to have $\frac{1}{10}$ of the velocity of the plasma at the wall.

Since the simulation is cylindrically symmetric, physically one would expect the gradient and flux of all quantities at the center boundary to be zero. This is the boundary condition set in UEDGE.

The top boundary represents the plasma-facing materials at the top of the gas box as well as outside the FRC core. Here, all of the plasma and atomic deuterium hit-

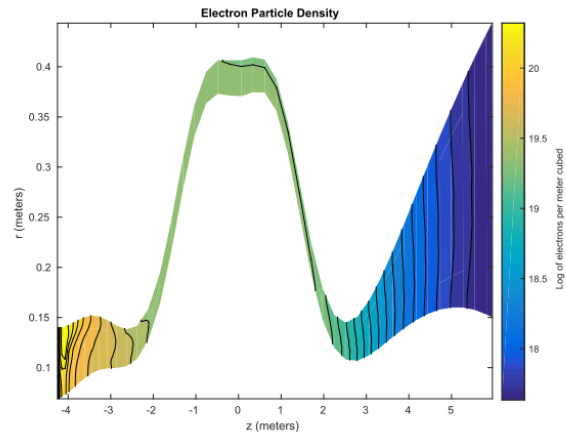


FIG. 3. Electron density for the representative case of 1MW heating power and 0.08 grams per second of gas input.

ting the top wall was recycled as molecular deuterium. An albedo of 0.5 was also set, meaning that the incoming atomic deuterium flux was reduced by a factor of 2. Zero temperature and velocity gradients were set at this boundary. Charged particle transport to these walls is negligible owing, in large part, to the rapid axial flow.

III. RESULTS

Heating power (0.5-4 MW) and gas input (0.01-0.5 grams per second) were varied to determine their impacts on the variables of interest.

A. SOL parameters

Figure 3 shows the electron density as a function of position for one simulation. The results for the values of 1MW and 0.08 grams per second are representative of typical results for these simulations. This density is exactly equal to the ion density. Notice that the plasma density is highest in the gas box region, roughly 10^{20} per m^3 , while the density is roughly 3×10^{19} surrounding the core and another order of magnitude lower in the expansion region.

Figure 4 shows the electron temperature for the representative simulation. Notice that the temperature is lowest in the gas box, around 1-5 eV, peaks around the core (20-25 eV), and cools to 15 eV in the expansion region.

Figure 5 shows the ion energy per particle for the representative simulation. Notice that the ion energy per particle rises from about 20eV per particle to about 120eV per particle in the expansion region. This increase in energy is driven by a significant increase in the kinetic energy of the ions. Figure 6 shows the z-component of the velocity of the ions (which is exactly equal to the velocity

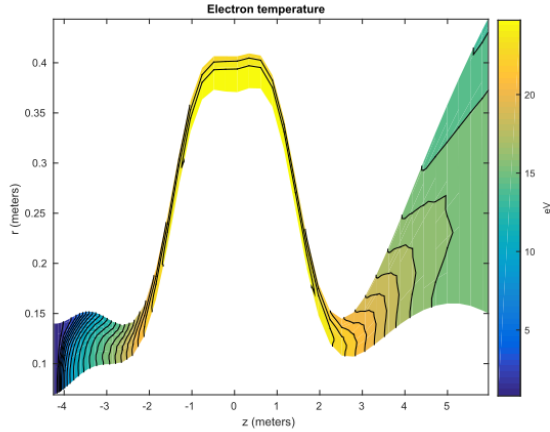


FIG. 4. Electron temperature for the representative case of 1MW heating power and 0.08 grams per second of gas input.

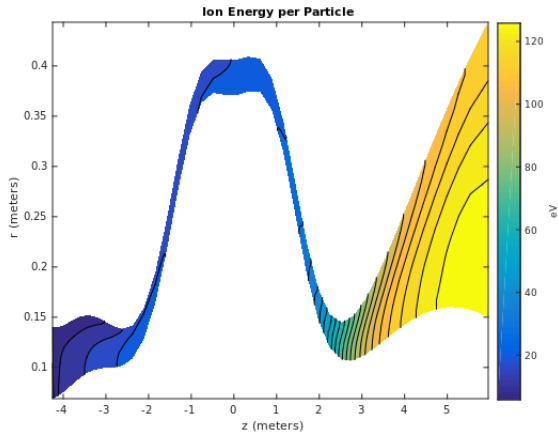


FIG. 5. Ion energy per particle (thermal and kinetic) for the representative case of 1MW heating power and 0.08 grams per second of gas input.

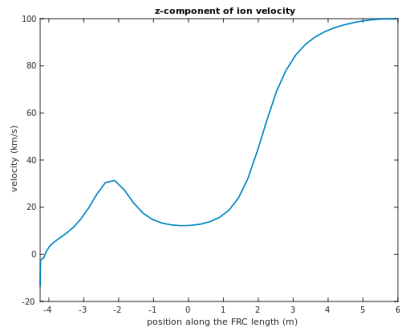


FIG. 6. z-component of ion velocity for the representative case of 1MW heating power and 0.08 grams per second of gas input.

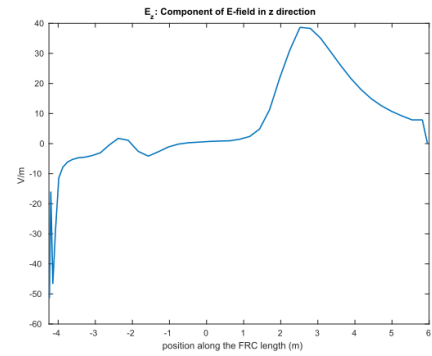


FIG. 7. z-component of electric field for the representative case of 1MW heating power and 0.08 grams per second of gas input.

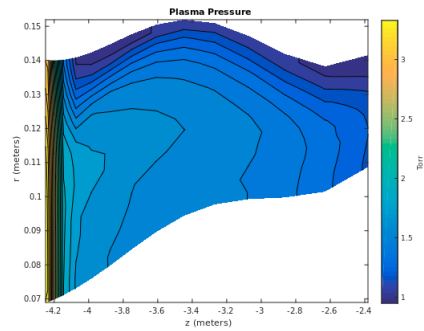


FIG. 8. Plasma pressure in the gas box for the representative case of 1MW heating power and 0.08 grams per second of gas input.

of the electrons. Figure 7 shows the z-component of the electric field along a field line. Here, the electric field is positive in and beyond the magnetic nozzle. This electric field arises due to the higher electron thermal flux out the nozzle, and serves to transfer electron thermal energy to ion kinetic energy.

B. Gas box analysis

Figure 8 shows the plasma pressure (sum of ion, electron, and neutral pressures) in the gas box for the representative case of 1MW and 0.08 grams of gas input per second. Notice that the pressure gradient (peaked near $r = 0.11$ cm) is parallel to the magnetic field. This gradient drives the plasma flow out of the gas box. Figure 9 shows the electron temperature for this case. Notice that the electrons are much cooler at the gas box wall ($1eV$) than inside the gas box.

Figure 10 shows the plasma pressure in the gas box for a different simulation, this time with 1MW of heating power and 0.05 grams per second of gas input. Notice that the pressure gradient parallel to the magnetic field is much smaller. Figure 11 shows the electron temperature

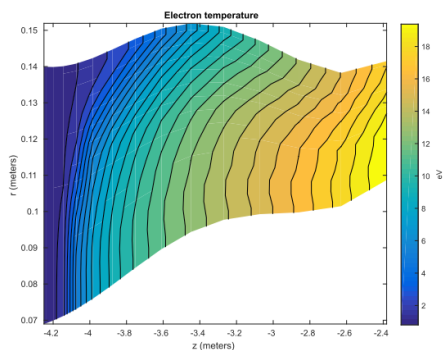


FIG. 9. Electron temperature in the gas box for the representative case of 1MW heating power and 0.08 grams per second of gas input.

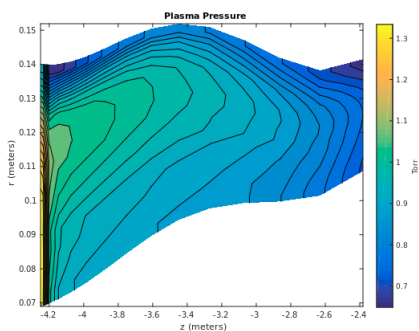


FIG. 10. Plasma pressure in the gas box for the case of 1MW heating power and 0.05 grams per second of gas input.

for this simulation. Notice that the electrons are warmer (5-10eV) near the gas box wall than those in Fig. 9.

Here, "Gas Box" is defined as the left boundary of the simulation ($z = -4.2m$) and "Wall" is defined as the top boundary of the simulation (maximum r for a given z). The power flow to material surfaces as a function of gas input and heating power is shown in figures 12, 13, and 14.

As the gas input is increased from 0.05 grams per sec-

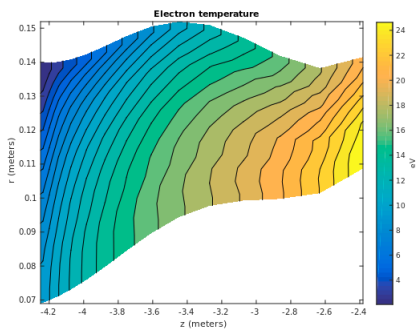


FIG. 11. Electron temperature in the gas box for the case of 1MW heating power and 0.05 grams per second of gas input.

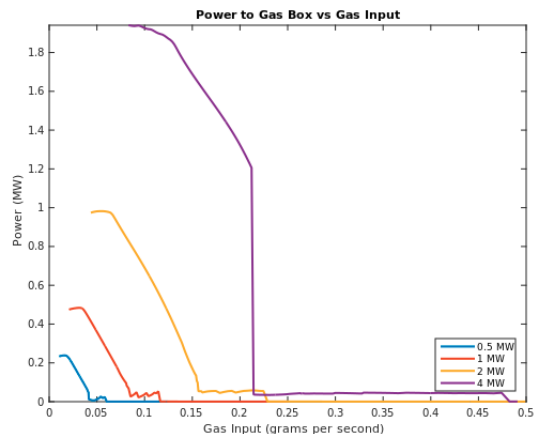


FIG. 12. Power flow to the gas box wall (the wall at $z = -4.2m$) as a function of heating power and gas input.

ond to 0.08 grams per second, the plasma transitions from an attached to a detached state. As expected for a detached state, the power to the gas box wall decreases significantly between 0.05 and 0.08 grams per second of gas input as well, as seen in figure 12.

The flat lines in figure 13 (and 14) are where the entire simulation has recombined into neutral gas. In this regime, all of the input power is transported radially as thermal neutral flux to the top wall. While the plasma is not recombined, the total power to material surfaces (figure 14) trends downwards, then flat, as the gas input increases. The flat region suggests that gas box detachment is stable, up to the point where the plasma recombines.

Using the velocity and density at the open end of the simulation, as well as generalized rocket equations, I calculated the thrust, specific impulse, and rocket efficiency as a function of heating power and gas input for this FRC. That data is shown in figures 15, 16, and 17. Not shown is the thermal energy of the ions and electrons flowing out of the magnetic nozzle, which accounts for as much as 30% of the input energy but does not factor into the rocket efficiency.

C. Rocket performance

IV. CONCLUSION

For a given heating power (which would be determined mainly by the size of the FRC), the gas input to the gas box determines whether the plasma in the gas box will be attached or detached. For low gas inputs, the plasma will remain attached, and the power to the gas box walls will be high. For higher gas inputs, the plasma will become detached, and the combined power to the gas box walls (end and top) will be lower. The fact that there exists a regime where the combined power to the gas box walls

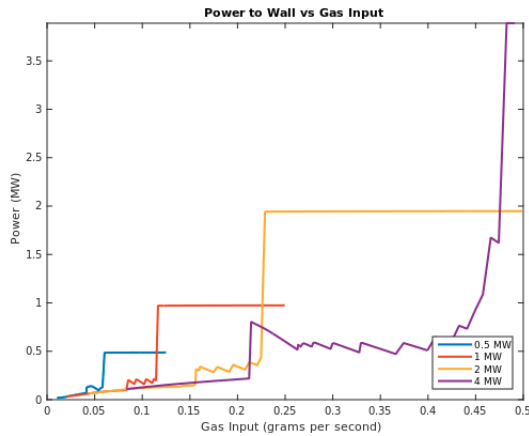


FIG. 13. Power flow to the outer wall (maximum r for a given z) as a function of heating power and gas input.

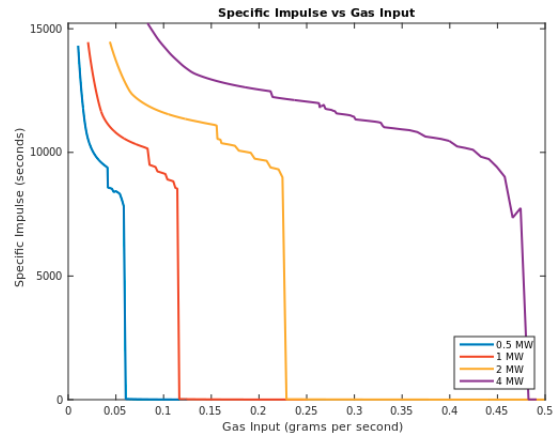


FIG. 16. Specific impulse as a function of heating power and gas input.

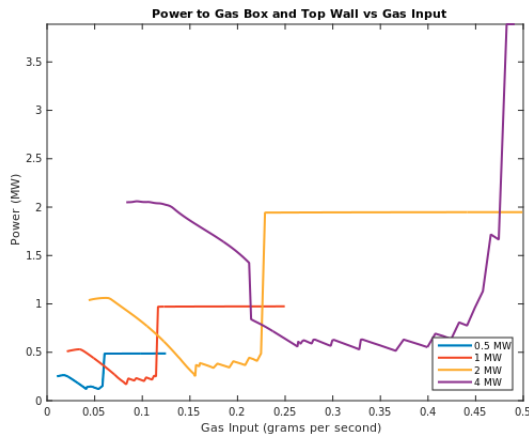


FIG. 14. The sum of power flow to the outer wall and the gas box wall as a function of heating power and gas input.

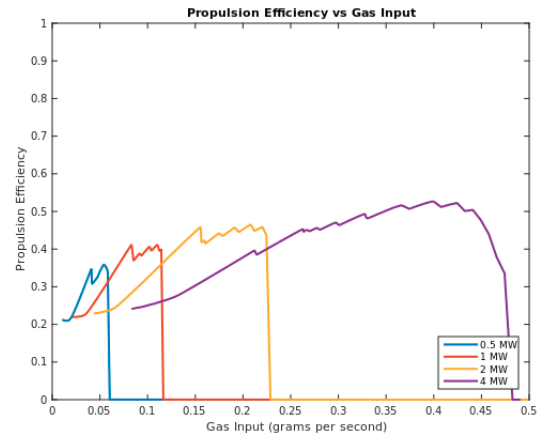


FIG. 17. Rocket efficiency as a function of heating power and gas input.

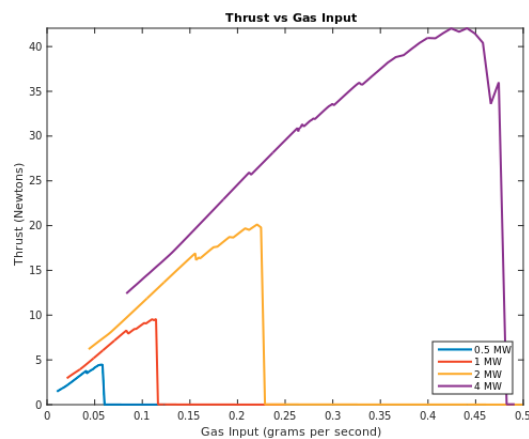


FIG. 15. Thrust as a function of heating power and gas input.

does not change appreciably with changes in gas input suggests that this detachment is stable. If the gas input becomes sufficiently high, the plasma will recombine.

For reactor and rocket applications, low power flux to and low ion impact energies on material surfaces is preferable to prevent damage to them. Therefore, a cold or even detached plasma state is desired. For a given heating power, these results suggest that there exists a range of optimal gas input values which would lead to detachment. Detached plasmas have been formed experimentally in power flow densities and gas pressure ranges similar to those discussed here.^{8,9,10}

For a given heating power, the gas input to the gas box determines the thrust value, specific impulse, and rocket efficiency. Until the plasma recombines, higher gas inputs correlate with higher thrust values, lower specific impulse values, and higher propulsion efficiency.

For rocket applications, in general high thrust, high specific impulse, and high rocket efficiency are desired.

These results suggest a trade-off between thrust and efficiency with specific impulse.

In particular, the calculated value of approximately $10N$ of thrust for a heating power of 1MW is sufficient for high-speed space missions within the solar system. Therefore, these results suggest that an FRC would be well-suited for use as a direct-fusion drive rocket.

V. ACKNOWLEDGEMENTS

I'd like to thank Dr. Sam Cohen for his support of me and of this project. He was consistently generous with his time and consistently insightful with his comments. I'd like to thank Eugene Evans for being my teacher and mentor throughout the summer. This project belongs to him as much as anyone. Amir Raja was a great partner for the three weeks we worked together, but he's an even better human being. I'm proud to call him my friend. I'd also like to thank Olivier Oizacard, Charles Swanson,

Tom Rognlien, and Bruce Cohen.

¹Wurden, G. A., Weber, T. E., Turchi, P. J., Parks, P. B., Evans, T. E., Cohen, S. A., . . . Campbell, E. M. (2015). A New Vision for Fusion Energy Research: Fusion Rocket Engines for Planetary Defense. *Journal of Fusion Energy*, 35(1), 123-133.

²Cohen, S. A., et al.

³G.S. Chu and S.A. Cohen, PRL 76, 1248 (1995)

⁴B. Cohen, T. Rognlien, LLNL, UEDGE Simulations of a 2D Nozzle

⁵Matthew Chu Cheong, et al. Energetic Particle Slowing in FRC Edge

⁶S.I. Braginskii, Transport processes in a plasma *Reviews of Plasma Physics*, Vol. I, Ed. M.A. Leontovich (Consultants Bureau, New York, 1965), p. 205.

⁷Matthew Chu Cheong, Analysis of Heat and Particle Flows in the Scrape-Off Layer of a Field-Reversed Configuration

⁸G.S. Chiu and S.A. Cohen, Phys. Rev. Lett. 76:8 (19 February 1996) 1248-1251.

⁹G.S. Chiu and S.A. Cohen, Phys. Plasmas 3:11 (November 1996) 4250-4267.

¹⁰Jaeyoung Park, T.K. Bennett, M.J. Goekner, and S.A. Cohen, J. Nucl. Mater. 241-243 (11 February 1997) 489-493.